Surface functionalization of carbon fibers with active screen plasma

Corujeira Gallo, Santiago; Charitidis, Constantinos; Dong, Hanshan

DOI:
10.1116/1.4974913

Surface functionalization of carbon fibers with active screen plasma

Santiago Corujeira GalloConstantinos CharitidisHanshan Dong

Citation: J. Vac. Sci. Technol. A **35**, 021404 (2017); doi: 10.1116/1.4974913
View online: http://dx.doi.org/10.1116/1.4974913
View Table of Contents: http://avs.scitation.org/toc/jva/35/2
Published by the American Vacuum Society

Surface functionalization of carbon fibers with active screen plasma

Santiago Corujeira Gallo[a)]
School of Metallurgy and Materials, University of Birmingham, Edgbaston, Birmingham B15 2TT, United Kingdom

Constantinos Charitidis
School of Chemical Engineering, National Technical University of Athens, Iroon Polytechniou 9, Zografou 157 80, Greece

Hanshan Dong
School of Metallurgy and Materials, University of Birmingham, Edgbaston, Birmingham B15 2TT, United Kingdom

(Received 3 October 2016; accepted 11 January 2017; published 24 January 2017)

The active screen plasma technology was used to functionalize carbon fibers and vitreous carbon disks. The plasma treatment conditions were mapped using optical emission spectroscopy and the functionalized surfaces were analyzed using scanning electron microscopy and atomic force microscopy, x-ray photoelectron spectroscopy, and contact angle measurements. A relationship was found between the active species in the plasma and the functional groups attached to the carbon surfaces, which provides valuable information for the optimization of the active screen plasma treatment. Moreover, the surface analyses were repeated over a period of 28 days to study the aging of the functionalized surfaces in air. The hydrophobic recovery was modeled using a surface restructuring theory which revealed a mean lifetime of 3.4 days for the functional groups. © *2017 American Vacuum Society*. [http://dx.doi.org/10.1116/1.4974913]

I. INTRODUCTION

Carbon fibers (CFs) are exceptional reinforcements for polymer matrix composites. The fibers exhibit high specific strength and stiffness, thermal stability, and corrosion resistance.[1] CF composites allow significant weight reductions, which make them attractive materials for aerospace, transportation, and wind power applications, among others. The properties of carbon fiber reinforced polymers (CFRP) depend, to a large extent, on the interaction between the strong CFs and the soft polymer matrix, most frequently an epoxy resin. Therefore, several strategies have been explored to modify the surface of CFs in order to improve the nature of the interface,[2,3] including:

(1) removing contaminants and weakly bonded layers from the surface of the CFs;
(2) applying a binder or a coupling agent;
(3) increasing the surface roughness to promote mechanical interlocking;
(4) attaching functional groups to increase the compatibility with the polymer.

A large number of techniques have been reported to modify the surface of CFs, ranging from the wet chemical processes[4–6] to sophisticated RF plasmas,[7] electron beam irradiation,[8] and multistep treatments.[9] However, some of these processes reduce the tensile strength of the fibers, while others are complex, expensive, or inappropriate for large scale implementation. Therefore, there is a need for a simple and effective technique to functionalize CFs, and nonthermal plasmas are attractive because of environmental and technical reasons.[10]

The interaction between the active species in the plasma and the carbon surface determines the type of functionalization. With this regard, the surface structure of the CFs affects the attachment of functional groups.[11] Low-modulus fibers have a less-ordered structure, and the dangling carbon bonds offer preferential sites for functional groups to attach.[12] On the other hand, high-modulus fibers have a high degree of alignment and the exposed graphitic basal planes are very inert. In spite of this, plasma treatments are capable of functionalizing graphitic surfaces by creating active sites through mild ion etching.[13]

The gases used for plasma functionalization of CFs include oxygen, argon, nitrogen, ammonia, and several hydrocarbons.[3] Ammonia (or the equivalent nitrogen-hydrogen gas mixture) is particularly interesting because the $-NH_x$ groups create strong bonds with the epoxy resins used in CFRPs.[3,10,13] At the same time, ammonia (or N_2-H_2) plasmas produce a mild ion etching, which creates active sites while minimizing the surface damage. The excessive increase in roughness and the creation of surface defects which reduce the mechanical properties of the CFs are important barriers for the uptake of surface treatments.[11]

Active screen (AS) is an advanced plasma technology developed in the early 2000s.[14] The experimental set up has been described elsewhere,[15] and the benefits of the AS technology are related with the exposure of the treated surfaces to active species in the plasma, with minimum or no damage by ion bombardment. In recent years, the AS technique was used to functionalize polymers with N_2-H_2 plasmas,[16] and a preliminary study showed potential for the successful functionalization of carbon surfaces, mainly carbon fibers.[17]

In this study, the AS plasma technology was used to functionalize CFs with N_2-H_2 gas mixtures. The processing

a)Electronic mail: corujeis@bham.ac.uk

TABLE I. Nominal properties of Toray carbon fibers T-700-12 k-60E (from spec sheet).

Strength (GPa)	Modulus (GPa)	Strain (%)	Yield (g/1000 m)	Density (g/cm^3)	Diameter (μm)	Sizing type	Sizing volume
4.9	230	2.1	800	1.80	7	60E	0.3%

conditions were optimized for the treatment of carbon surfaces, and the discussion relates the active species identified in the plasma with the surface chemistry measured on the functionalized CFs and the resulting contact angle. Some observations about the aging of the functionalized surfaces in air are also presented and discussed.

II. EXPERIMENT

A. Carbon fibers

T-700 carbon fibers were acquired from Torayca and the physical and mechanical properties of the fibers are summarized in Table I. A segment of the yarn, approximately 50 cm long, was coiled inside a cellulose thimble, and the fibers were cleaned with acetone for 24 h using a Soxhlet glassware; the volume of the thimble was filled with freshly condensed acetone every 3 min.[18] The fibers were subsequently transferred to a clean glass beaker and dried inside an oven for 7 h at 80 °C. The clean and dry fibers were stored in a vacuum desiccator.

Short segments of CF were fixed onto holders made of stainless steel foil (15 × 10× 0.1 mm) using double sided copper tape for scanning electron microscopy (SEM). The stainless steel foil holders had a 5 mm hole punched at the center, where the fibers could be analyzed with minimum background signal [Fig. 1(a)]. The holders also fitted tightly inside glass vials, so that the fibers fixed onto them would not touch the inner surfaces, thus avoiding contamination.[19] Small pieces of aluminum foil were used as plugs, to limit the movement of the foil along the vial.

B. Vitreous carbon disks

A vitreous carbon rod, 6 mm in diameter and 100 mm long, was acquired from Almath Crucibles Ltd. (VCR6100). Disks 6 mm in diameter and 1 mm thick were extracted from the rod using a Struers Accutom precision cut-off machine, fitted with an Al_2O_3 blade and circulating abundant cooling fluid. The disks were ground with wet abrasive papers #1200, #2500, and #4000, and polished with colloidal silica suspension (Struers OP-S). Finally, the polished disks were sonicated in acetone for 10 min and dried with cold air [Fig. 1(a)].

C. Active screen plasma treatments

The plasma treatments were conducted inside a Klockner Ionon 60 kW DC plasma furnace, where an AS arrangement was prepared [Fig. 1(b)]. The cathodic mesh of the AS set-up was made of austenitic stainless steel, with 6 mm holes, disposed in a staggered arrangement, and a distance of 10 mm between centers. The vitreous carbon disks and the pieces of stainless steel foil, with the carbon fibers attached onto them, were placed on an insulated work table, which was left at floating potential during the plasma treatment. The distance between the samples and the lid of the AS set-up was 15 mm. The temperature was monitored using a K-type thermocouple inserted in a dummy block and remained below 100 °C in all cases.

The vacuum chamber of the furnace was evacuated to a base pressure below 1 Pa, at which point a gas mixture consisting of 25% N_2 and 75% H_2 was fed into the chamber at a flow rate of 4 l/h. The glow discharge was ignited between the mesh of the AS set-up, which was connected to the cathode, and the vacuum chamber of the furnace, which was grounded. The gas pressure selected for the treatments was 50 Pa, the applied potential was between 200 and 400 V, the current was limited to 1 A, and the treatment time ranged from 5 to 40 min.

D. Optical emission spectroscopy

Optical emission spectra were acquired for different processing conditions using a Jobin Yvon Triax 180 monochromator, fitted with a 150 grooves/mm grating. The SPECTRAMAX for Windows software was used to control the monochromator and to collect the optical signal. The integration time was 30 s, and the slit width was 0.2 mm. The input optics consisted of a fused silica optical fiber (UV-Vis multimode), with a core diameter of 200 μm and a doped silica cladding 10 μm thick

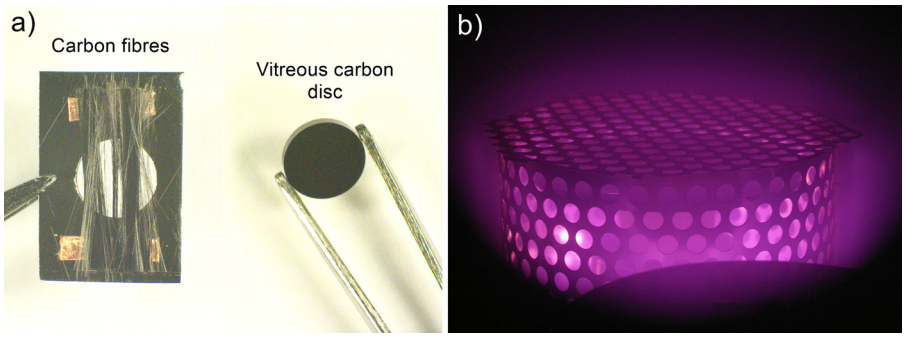

FIG. 1. (Color online) (a) Macrograph of the specimens used for characterization and (b) active screen experimental set-up.

and a polyimide buffer (AMS Technologies SFH200/220/245T). The fiber was fed into the vacuum chamber through a sealed aluminum flange (custom made feedthrough for optical fibers), and the tip was placed in close proximity to the samples, inside the AS experimental set-up. The data sets were collected at cathodic potentials between 200 and 400 V and at gas pressures between 25 and 125 Pa. The measurements were acquired in duplicates, and two separate runs were conducted, giving a total of four measurements per treatment condition. The active species were identified using the PLASUS SPECLINE v1.3 software.

E. Characterization

The surface morphology of the plasma treated fibers was observed using a JEOL-7000 FEG SEM and a Veeco MultiMode atomic force microscope (AFM), fitted with a SiN cantilever for contact mode. The elastic constant of the selected tip was 0.12 N/m.

The surface composition was assessed by x-ray photoelectron spectroscopy (XPS) in a Thermo Scientific K-Alpha instrument with a monochromatic source (1486.6 eV, 12 kV, and 3 mA anode current). The spot size used was 400 μm, and the pass energy values were 200 eV for the survey spectra and 40 eV for the high-resolution scans, C (1s), N (1s), and O (1s). Three data sets were collected for each specimen, and all spectra were calibrated using the C (1s) sp^2 reference peak (284.5 eV) and subsequently added. The resulting spectra were analyzed using CASA XPS version 2.3.16. The relative sensitivity factors were 1.00 for C, 1.80 for N, and 2.93 for O. The synthetic peak models were obtained using a Tougaard background and Gaussian-Lorentzian peak shapes. The components considered for the models are listed in Table II. Several XPS measurements were conducted over a period of 1 month, in order to determine the degradation or aging of the functionalized surfaces in air.

F. Wettability

The contact angle measurements were obtained in an Attension optical tensiometer, from Biolin Scientific, using the sessile droplet method with deionized (DI) water. The quantitative assessment of wettability on single filaments of CF proved to be very challenging. Several attempts were made to measure the contact angle of microdroplets on carbon fibers using different liquids: water, glycerol, ethylene glycol, tetradecane, etc. These attempts failed because it was difficult to form droplets of consistent size on single carbon fibers and, in some cases, the liquid evaporated too quickly so that the size and shape of the small droplets changed during the measurement. Therefore, vitreous carbon disks were used as proxies of CFs for the contact angle measurements.[21] Even though the density of active sites on vitreous carbon disks may differ from that on CFs, the relative trends observed in both cases are expected to be very similar, particularly regarding the degradation or aging of the functional groups in air.

To conduct these measurements, a small droplet (0.5 μl) was suspended from the needle of the tensiometer and slowly brought in contact with the surface of the vitreous carbon disks. The volume of the droplet was subsequently increased to 2 μl, and the needle was carefully withdrawn before the images were collected. The contact angle was measured automatically using the ONEATTENSION software (v2.5), and the reported values are the average of at least three separate measurements. The assessment includes several tests conducted over a period of 1 month after the plasma treatment, in order to determine the degradation or aging of the functionalized surfaces in air.

III. RESULTS

A. Optical emission spectroscopy

The typical optical emission spectrum collected during the AS plasma treatments is illustrated in Fig. 2. In all cases, the emission spectra were dominated by the emission lines/bands corresponding to H_α (656.3 nm) and N_2^+ (391.4 nm) ions, followed by the N_2^* (313.6 nm), NH (337.0 nm), and H_2 excited species.[22] The intensity of the peaks corresponding to nitrogen containing species was normalized with respect to the H_α peak for the purpose of comparison.

The results recorded for different AS plasma conditions are summarized in Table III. In general, the emission intensity was directly proportional to the applied voltage and inversely proportional to the gas pressure. On the other hand, the relative intensity of the N_2^* and NH excited species showed the opposite trend. This is noteworthy because the

TABLE II. List of component peaks considered for the XPS model (Ref. 20).

C (1s)		N (1s)		O (1s)	
Binding energy [eV]	Component peak	Binding energy [eV]	Component peak	Binding energy [eV]	Component peak
284.4–284.6	C sp^2	398.4–399.0	Pyridine	531.2–531.4	−C=O
284.9–285.1	C sp^3	399.4–399.8	Amines, amides	532.0–532.2	C=O
284.8–285.0	C-COOH	400.1–400.7	Pyrroline, pyridone	532.7–532.9	-OH, C-O-C
285.4–285.6	C-N	401.1–401.7	Pyridinium	533.5–533.7	-OH, C-O
286.1–286.4	C-O-H, C≡N	403.7–404.3	Shake up	534.8–535.2	Chemisorbed H_2O
287.4–287.6	C=O	405.5–405.7	NO_x	536.2–536.6	Physisorbed H_2O
288.3–288.9	COOH			538.2–538.6	Shake up
290.1–290.5	Physisorbed H_2O				
291.3–291.7	Shake up				

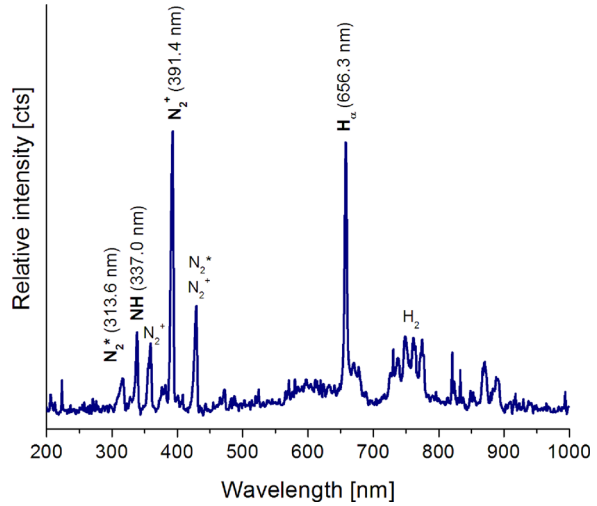

FIG. 2. (Color online) Typical optical emission spectrum observed in the AS plasma treatments.

surface functionalization is frequently attributed to such excited molecules, and the emission intensity is a measure of the abundance of the species in the plasma. Therefore, the identification of suitable plasma conditions to form the appropriate active species in the plasma is important for the optimization of the process.

B. Surface chemistry

The typical survey spectra obtained by XPS on untreated (UT) and AS plasma treated CFs are illustrated in Figs. 3(a) and 3(b), respectively. The main resonance peaks are labeled C (1s), N (1s) and O (1s). The peaks observed at higher binding energy were attributed to Auger effect, whereas the two minor peaks at 100 eV and 150 eV, which appeared in all the specimens without a clear trend, were attributed to Si contamination. The quantified data are summarized in Table IV.

The results in Table IV reveal an increase in the nitrogen content of the CFs after the AS plasma treatments. It is interesting to note that, for a given treatment time (e.g., 20 min), the nitrogen content shows an inverse correlation with the applied voltage, which is in agreement with the abundance of N_2^* and NH excited species measured by optical emission spectroscopy (OES). Iron was also detected on the surface of the CFs plasma treated at higher voltage or for longer times (20–40 min). This is attributed to the sputtering of material from the mesh of the AS set-up and its subsequent redeposition on the CFs. The iron deposited on the CFs exhibited varying degree of oxidation (FeO, Fe_2O_3, F_3O_4, and FeOOH), which accounts for the higher oxygen content observed on these specimens.

The high-resolution spectra corresponding to the C (1s), N (1s), and O (1s) regions of the UT and AS plasma treated CFs are shown in Fig. 4. The C (1s) spectrum of the UT CF exhibits a peak of C-O-R groups, which is attributed to residues of the binder agent (sizing) left on the surface after the cleaning procedure; the amount of binder is small, judging by the peak shape. The main changes in the C (1s) spectrum after the AS plasma treatment are observed in the high-energy tail, particularly related with an increase in the content of COOR functional groups.

The most noticeable change in the spectrum was observed in the N (1s) region, where the intensity of the signal increased after the AS plasma treatment, and the shape of the peak changed considerably. The difference was attributed to the introduction of several N and N-H groups,[20,23] mainly amine and pyridone. The O (1s) region of the scan exhibited a broadening toward the low-energy tail of the peak, which was attributed to the quinone (–C=O) and ester (C=O) components. The samples treated at higher power and longer times also exhibited oxygen peaks associated with iron oxides.

The XPS analysis was repeated at regular time intervals on one same specimen, and the results are illustrated in

TABLE III. Emission intensity of active species for different AS plasma processing conditions.

AS parameters		Emission intensity (cts)				Relative intensity (%)		
Pressure [Pa]	Potential [V]	N_2^* (313.6 nm)	NH (337.0 nm)	N_2^+ (391.4 nm)	H_α (656.8 nm)	N_2^*/H_α	NH/H_α	N_2^+/H_α
25	200	14499	16177	22751	24309	60	67	94
	300	14925	16736	25647	26934	55	62	95
	400	19094	25734	65535[a]	65535[a]	29	39	N/A
50	200	15262	17624	20618	21841	70	81	94
	300	14925	16736	25647	26934	55	62	95
	400	17385	22573	48770	50407	34	45	97
75	200	14468	15820	18618	20222	72	78	92
	300	17037	22939	38754	41124	41	56	94
	400	18454	27193	44871	47898	39	57	94
100	200	14977	17268	17382	18940	79	91	92
	300	18276	27361	37756	41223	44	66	92
	400	17942	26245	38050	41972	43	63	91
125	200	14375	16174	14938	16022	90	101	93
	300	16619	24522	24190	26316	63	93	92
	400	16559	24683	26292	28217	59	87	93

[a]These measurements reached the saturation limit of the detector; however, the width of the peak at such intensity was only a few pixels, so the real intensity was very close the saturation limit.

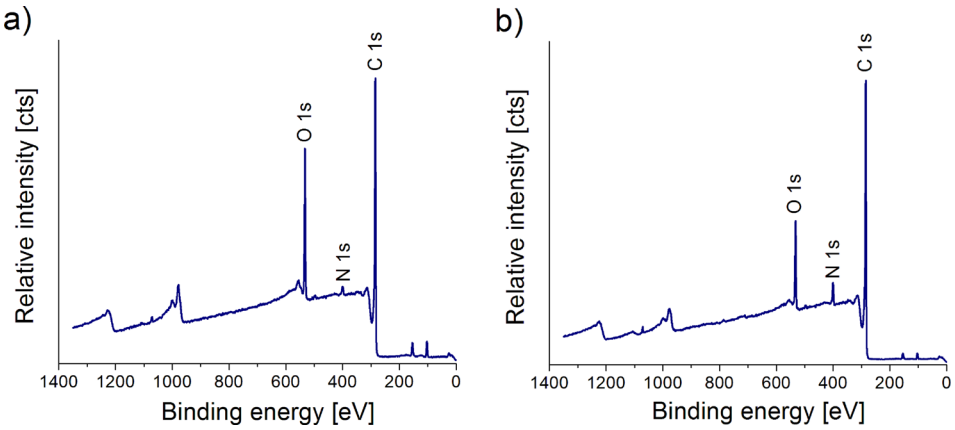

FIG. 3. (Color online) X-ray photoelectron spectra corresponding to (a) untreated and (b) AS plasma treated carbon fiber (300 V, 5 min).

Fig. 5. Once again, the most evident changes were observed in the N (1s) region of the spectrum. The synthetic peak revealed a considerable reduction of the amine component and a split between the pyridine and pyridone components, which shows a trend toward the shape observed on the untreated CFs. The chemical analysis conducted on the survey scans revealed a slow but consistent decrease in the nitrogen content over a period of 28 days, from 5.8 to 5.1 at. %. No significant change in the oxygen signal was detected.

Unfortunately, the first XPS measurement (t_0) was conducted approximately 2–3 weeks after the plasma treatment, so the chemical composition immediately after the treatment could not be assessed. Further discussion is given in Sec. IV B.

C. Wettability

Contact angle measurements were conducted on vitreous carbon disks, plasma treated alongside the CFs. Figure 6 shows the water droplets on carbon disks treated under different conditions. Increased wettability was obtained in all cases, but the most significant changes were observed on those specimens which were plasma treated at low potential (<300 V) and for short times (<20 min). Moreover, the micrographs in Fig. 4 were taken three days after the plasma treatment, and subsequent measurements were conducted within 1 h of the surface treatment revealed contact angles as low as 10°.

The evolution of the contact angle over time was significant, and the changes are illustrated in Fig. 7. The untreated carbon disks exhibited a high contact angle with deionized water, which is characteristic of hydrophobic surfaces. After the AS plasma treatment (300 V for 5 min), the contact angle dropped dramatically to values as low as 10°. However, the samples exhibited a hydrophobic recovery over time, as the plasma treated surface was exposed to atmospheric conditions. The progression was very rapid in the first few hours or days after the plasma treatment, but it became slower after 1 week and the contact angle finally stabilized at approximately 70°, which is slightly lower than the untreated material.

It is important to mention that the measurements were conducted both on pristine samples and on one same specimen at several aging times. For a given aging time, the specimens used for multiple measurements exhibited marginally higher contact angles than the pristine specimens, which had contact with the water for the very first time; but the difference was within the experimental error. Therefore, it was concluded that the exposure to deionized water during the measurements only had a minor effect on the results, and the aging was mainly attributed to the exposure of the AS plasma treated surfaces to air.

TABLE IV. Summary of XPS results obtained from carbon fibers (at. %).

Condition	C (1s)	N (1s)	O (1s)	Fe (2p)
UT	84.82 ± 3.69	1.92 ± 0.15	13.66 ± 3.59	N/A
AS 200 V 20 min	80.36 ± 1.52	5.59 ± 0.24	13.87 ± 1.56	0.18 ± 0.02
AS 300 V 5 min	82.19 ± 2.17	4.90 ± 0.06	12.88 ± 2.19	0.03 ± 0.01
AS 300 V 20 min	79.52 ± 1.93	5.08 ± 0.24	15.21 ± 2.03	0.19 ± 0.02
AS 300 V 40 min	76.63 ± 0.69	5.88 ± 0.22	15.73 ± 0.14	1.76 ± 0.41
AS 400 V 20 min	67.78 ± 3.14	4.23 ± 0.17	23.40 ± 2.97	4.58 ± 0.35

D. Surface morphology

The surface morphology of the untreated and AS plasma treated CFs are illustrated in Fig. 8. A smooth and featureless surface was observed in all cases, and the changes introduced by the AS plasma treatment were very minor, even under the most severe treatment conditions. The absence of ion bombardment on the CFs is evident from the lack of surface defects or arcing damage. No obvious signs of intense chemical etching were observed either, and only the longitudinal grooves of the CFs appeared somewhat deeper after the plasma treatment. Therefore, the small changes in surface roughness were attributed to the mild chemical etching and the deposition of iron particles sputtered from the AS set-up. No changes in the surface morphology were observed upon aging in air.

IV. DISCUSSION

A. Active species responsible for the surface functionalization

A comparison of the OES and XPS data presented in Sec. III reveals a correlation between the excited species in

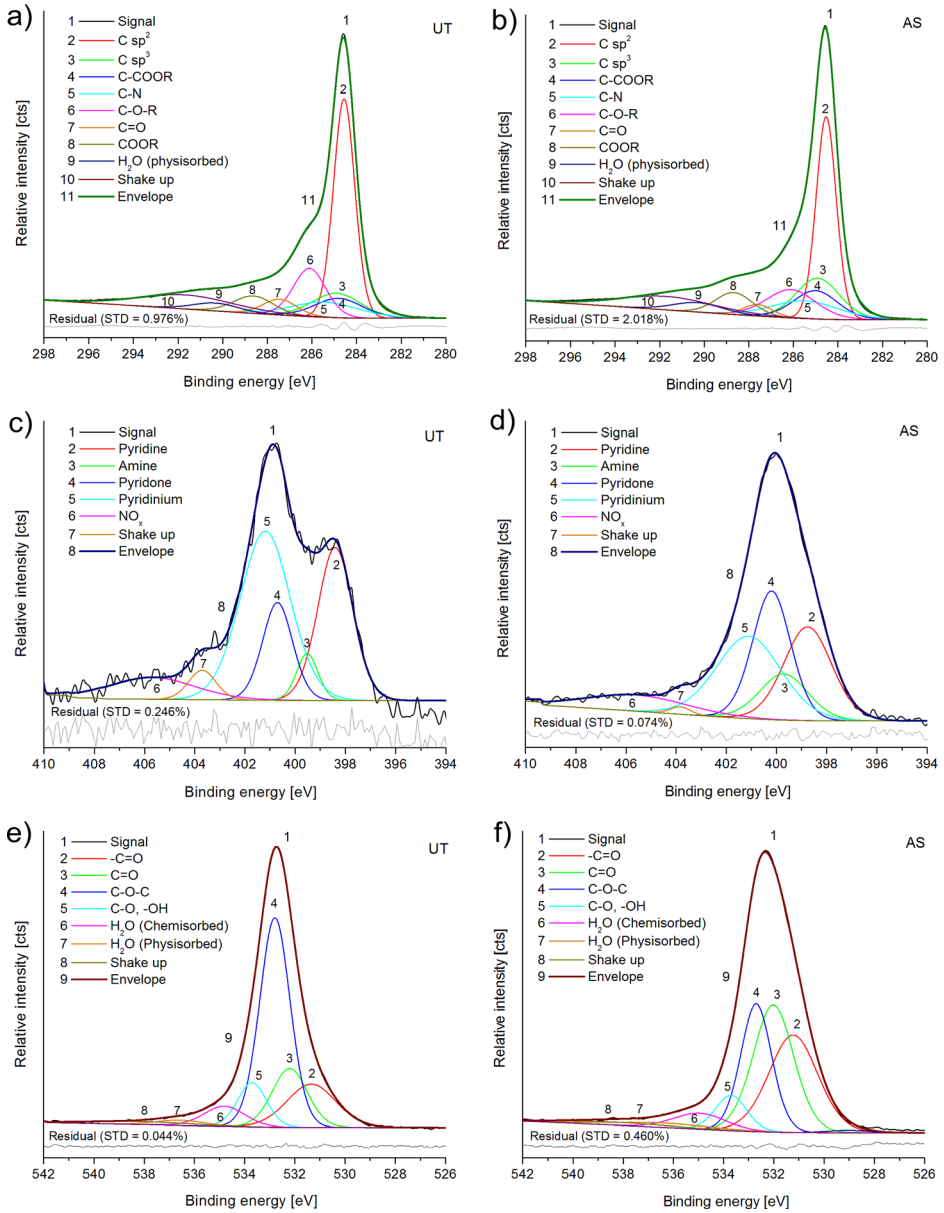

FIG. 4. (Color online): High resolution spectra for (a) and (b) C (1s); (c) and (d) N (1s); and (e) and (f) O (1s) corresponding to untreated (UT) and AS plasma treated carbon fibers.

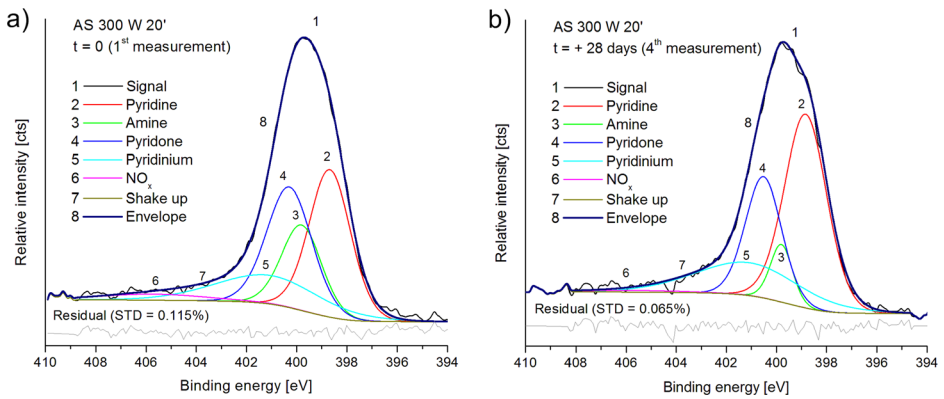

FIG. 5. (Color online) Evolution of the N (1s) peak over time for sample AS 300 V 20 min: (a) first measurement (t_0) and (b) fourth measurement (t_0 + 28 days).

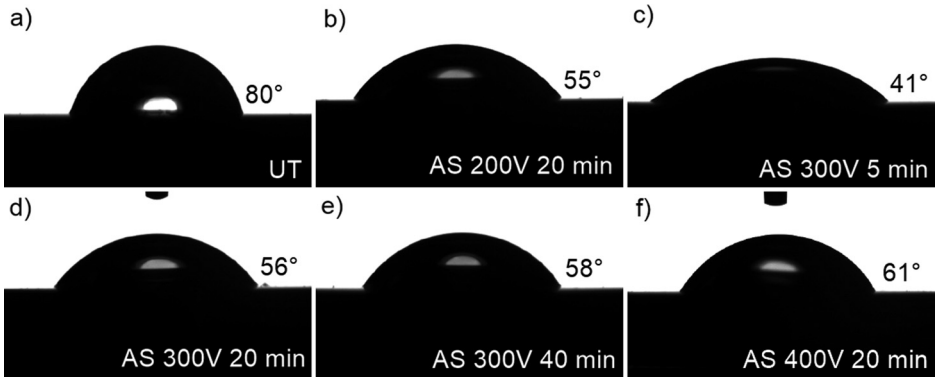

FIG. 6. Sessile droplets on vitreous carbon disks after AS plasma treatments under different conditions.

the plasma, particularly NH and N^*, and the nitrogen content on the surface of the plasma treated CFs (Fig. 9). It is interesting to note that the ionized species in the plasma, mainly N_2^+, showed no correlation with the nitrogen content on the CFs. Therefore, the functionalization of the carbon fibers may be linked to the excited species in the plasma, NH and N^*, rather than the ionized N_2^+ species.

Unfortunately, plasma diagnostic techniques have not been extensively used to characterize the plasma functionalization of CFs. However, several studies have been published on the surface functionalization of polymers with N_2-H_2 plasmas, and some observations may be extrapolated to carbon surfaces.[24] With regards to the attachment of nitrogen functionalities to the treated surface, particularly amine groups, other authors have reported a dependence on the applied power, gas mixture, and gas pressure.[24,25] The observed trend is similar to the one described in this study, with higher yield of nitrogen functionalities at low power and higher pressure.[26] The mechanism behind this correlation with the applied power has been attributed to changes in the plasma chemistry, mainly dissociation of N_2, H_2, and NH_2/NH_3 species at higher power.[24,26]

In addition to this, Favia *et al.*[24] suggested that there was a direct correlation between nitrogen functionalities grafted on the treated surface, and the N_2^* and NH active species in the plasma. This, however, does not exclude the role of other species, which may not be detected by OES. A high content of hydrogen in the gas mixture is also said to create active sites through a selective etching mechanism which facilitates the attachment of functional groups. In the case of carbon surfaces, a similar etching mechanism was reported by Yang *et al.*[27] for graphene exposed to a hydrogen RF plasma. The mild ion bombardment by positive ions was also said to create active sites for the attachment of functional groups.[12] However, this mechanism should be negligible in the AS arrangement, given that the CFs are kept at floating potential, and without cathodic bias.

On the other hand, the ionized N_2^+ species showed a direct correlation with the iron content measured on the fibers after the AS plasma treatment. This is attributed to the sputtering effect of energetic ions on the AS set-up, and the deposition of the sputtered material onto the exposed surfaces, including the CFs. The effect of such deposition layer on the CFs, and on the bond with the polymeric matrix in composite materials, has not been assessed yet. However, curing kinetic studies of epoxy resin modified with iron and iron oxide (Fe_2O_3) nanoparticles suggest that the iron deposition layer is likely to result in higher cross-linking density, glass transition temperature, thermal stability, and improved mechanical properties.[28,29]

B. Aging of functional groups attached to the surface of CFs

With regards to the contact angle measurements, Narushima *et al.*[30] reported that low power plasma treatments resulted in lower contact angles, thus following a similar trend to the functional groups attached on the surface. In the present study, the change in contact angle observed after the AS plasma treatment was remarkable. However, a hydrophobic recovery took place upon exposure of the specimens to air [Fig. 10(a)]. This behavior was observed in other materials, mainly polymers, although the rate of decay depended on the nature of the substrate, the plasma treatment conditions, and the aging environment.[31–34] In general, the change in chemistry and properties of the plasma functionalized surfaces is attributed to two factors, namely, surface oxidation upon reaction with atmospheric oxygen and surface adaptation through diffusion of surface species in the bulk,[35,36] although the latter mechanism is assumed to be negligible for carbon substrates.

The model proposed by Israelachvili and Gee[37] can be used to calculate the fraction of polar and nonpolar regions on plasma functionalized surfaces[38,39]

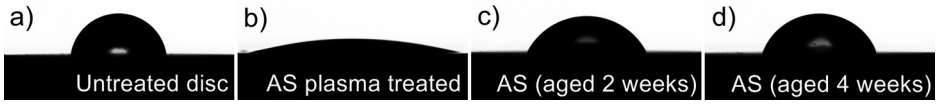

FIG. 7. Evolution of the contact angle after the AS plasma treatment at 300 V for 5 min. The samples were subsequently aged in air.

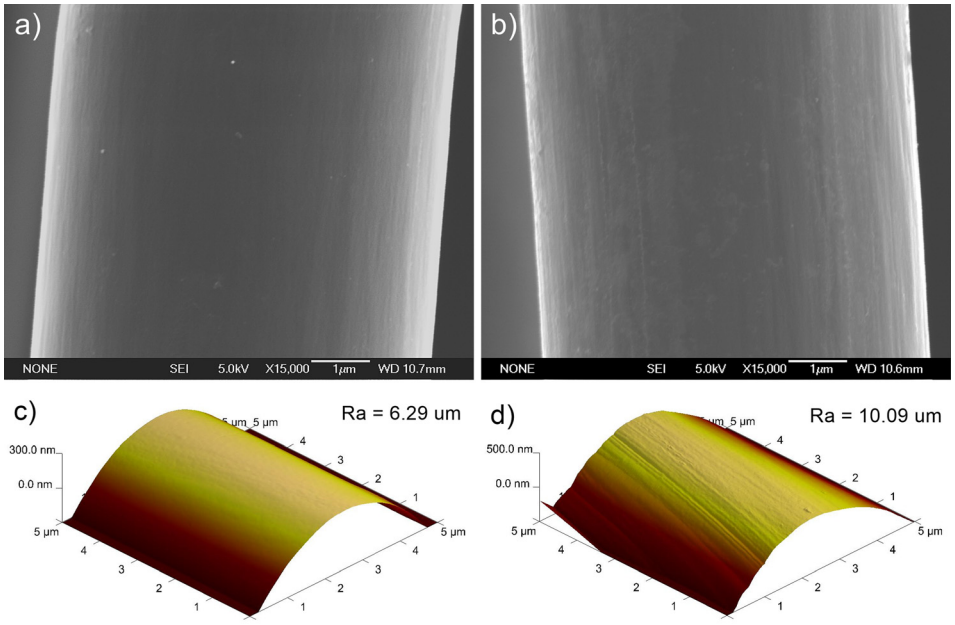

FIG. 8. (Color online) SEM micrographs and AFM surface plots of (a) and (c) untreated CF, (b) and (d) AS plasma treated CF (300 V, 20 min).

$$(1+\mathrm{Cos}\ \theta)^2 = f_p\,(1+\mathrm{Cos}\ \theta_p)^2 + f_{np}\,(1+\mathrm{Cos}\ \theta_{np})^2, \tag{1}$$

where θ is the equilibrium contact angle measured on the plasma treated surface, f_p is the fraction of the surface covered by polar regions, f_{np} is the fraction of the surface covered by nonpolar regions ($f_p = 1 - f_{np}$), θ_p is the equilibrium contact angle on a surface consisting of polar regions only (assumed to be 0°), and θ_{np} is the equilibrium contact angle on a surface consisting of nonpolar regions only (assumed to be 85°). Figure 10(b) shows the evolution of f_p with aging time. The initial value of f_p immediately after the plasma treatment is 97.5%, which correlates with the expected attachment of functional groups with N_2-H_2 plasma treatments. The lowest f_p value calculated after 28 days of aging in air was 17%, which illustrates the hydrophobic recovery described before. The change observed upon aging in air had an exponential decay form, described by

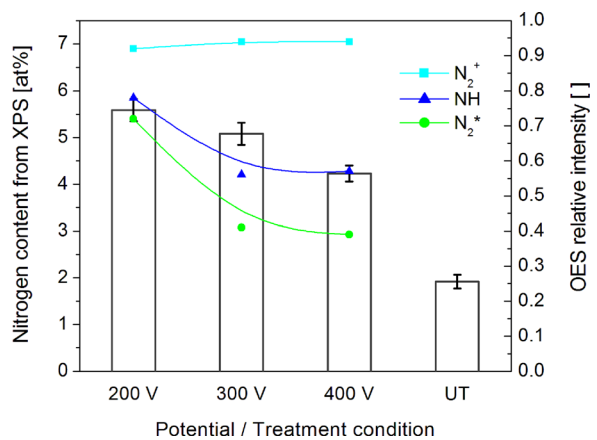

FIG. 9. (Color online) Correlation between the excited species in the plasma (OES) and the resulting nitrogen content on the carbon fibers (XPS).

$$f_p = y_0 + A_1 \cdot e^{-(x/\tau)}. \tag{2}$$

The fitting parameters and the quality of the fitting are reported in Table V. The fact that the experimental data can be modeled with an exponential decay function of the first order supports the previous assumption that the aging process may be attributed to one single physical mechanism, namely, the exposure of the plasma treated surface to air, while the diffusion of surface functionalities into the bulk material is negligible in this case. The value of τ in Eq. (2) represents the mean lifetime of the functional groups on the carbon surface, i.e., 3.4 days, and y_o is the residual value of f_p after aging, which in this case was 22%.

The AS plasma treated CFs exhibited a very similar surface morphology to the untreated fibers. The small differences were attributed to the mild chemical etching of hydrogen as well as the deposition of iron from the AS setup. In any case, no changes in surface morphology were observed over time. Therefore, there is no evidence to support that the changes in contact angle are associated with the topography of the carbon surfaces, and thus, the changes are mainly attributed to the surface chemistry.

The AS plasma treatments with a N_2-H_2 gas mixture clearly introduced polar functional groups on the carbon surfaces. This was reflected on the chemical composition measured by XPS and on the contact angle with DI water. However, the functional groups underwent an aging process when exposed to air. The contact angle could be measured within 1 h of the plasma treatment and at frequent time intervals over a period of 1 month. Therefore, this data set reflects the initial condition of the surface and its evolution over time with significant fidelity.

On the other hand, the first XPS measurement was conducted 2–3 weeks after the plasma treatment, when the functional groups had already degraded to some extent. As a

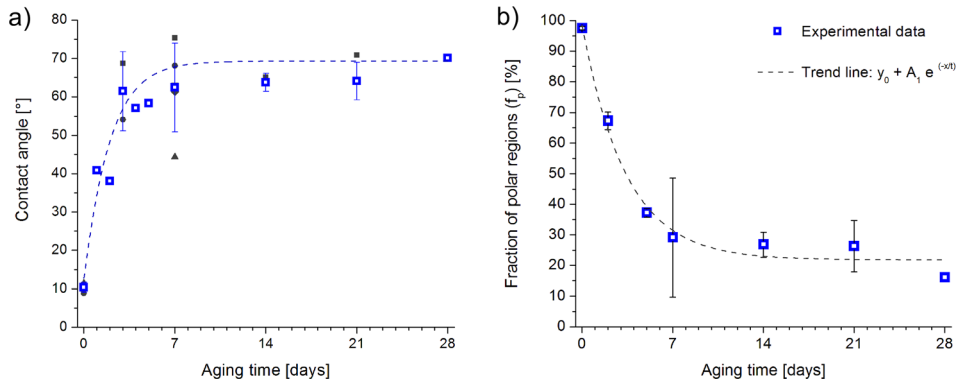

FIG. 10. (Color online) Evolution with aging time in air: (a) contact angle with DI water and (b) calculated fraction of polar regions.

consequence, the drop in nitrogen content observed in the XPS data set is attributed to the tail of the exponential decay described by Eq. (2). The extrapolation of the nitrogen content to the initial value using the lifetime (τ) and pre-exponential factor (A_1) in Table V revealed values as high as 80% immediately after the plasma treatment and 15% after 1 week.

The XPS results showed a decrease in the nitrogen content over time, but the oxygen content remained constant. Unfortunately, the degradation sequence is difficult to identify by XPS surface analysis because of technique limitations.[40] It is speculated that the NH functional groups undergo oxidative scissions and evaporative loss upon their exposure to air, although the elucidation of the degradation mechanism requires further study.

V. SUMMARY AND CONCLUSIONS

The functionalization of carbon fibers with the active screen plasma technology was successful. The surface of the CFs was enriched with nitrogen functional groups, which could be linked to NH and N^* excited species in the plasma. Furthermore, the map of processing conditions produced by OES provides general guidelines for future process optimization. With this regard, active screen plasma conditions combining low voltage and relatively high pressure are favorable for the formation of the excited species mentioned previously.

The active screen plasma treatment also produced a remarkable reduction in the contact angle of the carbon surfaces. However, the surfaces exhibited a hydrophobic recovery upon their exposure to air. The exponential decay, based on a surface restructuring model, revealed that the mean lifetime of the functional groups on the carbon surface is 3.4 days, and the residual fraction of polar regions after aging is 22%. The aging mechanisms remain unclear, but they seem to involve oxidative scissions and evaporative loss of nitrogen functional groups.

TABLE V. Fitting parameters for the exponential decay of f_p.

y_o	A_1	τ	R^2
21.799 ± 2.809	76.712 ± 5.088	3.376 ± 0.533	0.983

ACKNOWLEDGMENTS

The research leading to these results has received funding from the European Union's Seventh Framework Program (FP7/2007-2013) under the Agreement No. GA604248. X-ray photoelectron spectra were obtained at the National EPSRC XPS Users' Service (NEXUS) at Newcastle University, an EPSRC Mid-Range Facility.

[1]M. Sharma, S. Gao, E. Mäder, H. Sharma, L. Y. Wei, and J. Bijwe, Compos. Sci. Technol. **102**, 35 (2014).
[2]S. Tiwari and J. Bijwe, Procedia Technol. **14**, 505 (2014).
[3]B. Z. Jang, Compos. Sci. Technol. **44**, 333 (1992).
[4]C. U. Pittman, Jr., G. R. He, B. Wu, and S. D. Gardner, Carbon **35**, 317 (1997).
[5]F. Severini, L. Formaro, M. Pegoraro, and L. Posca, Carbon **40**, 735 (2002).
[6]L. H. Meng, Z. W. Chen, X. L. Song, Y. X. Liang, Y. D. Huang, and Z. X. Jiang, J. Appl. Polym. Sci. **113**, 3436 (2009).
[7]D. Akbar and T. E. Güngör, Surf. Coat. Technol. **240**, 233 (2014).
[8]L. Mao, Y. Wang, Z. Zang, S. Zhu, H. Zhang, and H. Zhou, J. Appl. Polym. Sci. **131**, 40274 (2014).
[9]Z. Chen, X. J. Dai, P. R. Lamb, J. du Plessis, D. R. de Celis Leal, K. Magniez, B. L. Fox, and X. Wang, Plasma Processes Polym. **10**, 1100 (2013).
[10]R. Morent, N. De Geyter, J. Verschuren, K. De Clerck, P. Kiekens, and C. Leys, Surf. Coat. Technol. **202**, 3427 (2008).
[11]L. G. Tang and J. L. Kardos, Polym. Compos. **18**, 100 (1997).
[12]C. Jones and E. Sammann, Carbon **28**, 515 (1990).
[13]C. Jones and E. Sammann, Carbon **28**, 509 (1990).
[14]J. Georges, U.S. patent 5989363 (23 November 1999).
[15]C. X. Li, T. Bell, and H. Dong, Surf. Eng. **18**, 174 (2002).
[16]X. Fu, M. J. Jenkins, G. Sun, I. Bertoti, and H. Dong, Surf. Coat. Technol. **206**, 4799 (2012).
[17]S. Corujeira Gallo, M. Koklioti, P. Jagdale, E. P. Koumoulos, H. Dong, A. Tagliaferro, and C. A. Charitidis, paper presented at the Carbon 2015, Dresden, 2015 (unpublished).
[18]ISO-BSI, *10548: Carbon Fibre—Determination of Sizing Content* (ISO, London, 2003).
[19]ISO-BSI, *18117: Surface Chemical Analysis—Handling of Specimens Prior to Analysis* (ISO, London, 2009).
[20]F. Vautard, S. Ozcan, F. Paulauskas, J. E. Spruiell, H. Meyer, and M. J. Lance, Appl. Surf. Sci. **261**, 473 (2012).
[21]J. B. Donnet and G. Guilpain, Carbon **27**, 749 (1989).
[22]R. W. B. Pearse and A. G. Gaydon, *The Identification of Molecular Spectra*, 3rd ed. (Chapman & Hall Ltd, London, 1963).
[23]J. R. Pels, F. Kapteijn, J. A. Moulijn, Q. Zhu, and K. M. Thomas, Carbon **33**, 1641 (1995).
[24]P. Favia, M. V. Stendardo, and R. D'Agostino, Plasmas Polym. **1**, 91 (1996).
[25]K. Narushima, M. Fukuoka, H. Kawai, N. Inagaki, Y. Isono, and M. R. Islam, Jpn. J. Appl. Phys., Part 1 **46**, 7855 (2007).

[26]A. A. Meyer-Plath, K. Schröder, B. Finke, and A. Ohl, Vacuum **71**, 391 (2003).
[27]R. Yang, L. Zhang, Y. Wang, Z. Shi, D. Shi, H. Gao, E. Wang, and G. Zhang, Adv. Mater. **22**, 4014 (2010).
[28]O. Zabihi, M. Aghaie, and K. Zare, J. Therm. Anal. Calorim. **111**, 703 (2013).
[29]T. Sun, H. Fan, Z. Wang, X. Liu, and Z. Wu, Mater. Des. **87**, 10 (2015).
[30]K. Narushima, N. Yamashita, Y. Isono, M. R. Islam, and M. Takeuchi, Jpn. J. Appl. Phys., Part 1 **47**, 3603 (2008).
[31]W. J. Brennan, W. J. Feast, H. S. Munro, and S. A. Walker, Polymer **32**, 1527 (1991).
[32]A. Jordá-Vilaplana, L. Sánchez-Nácher, D. García-Sanoguera, A. Carbonell, and J. M. Ferri, J. Appl. Polym. Sci. **133**, 43040 (2016).
[33]S. H. Lee, W. C. Lin, C. H. Kuo, M. Karakachian, Y. C. Lin, B. Y. Yu, and J. J. Shyue, J. Phys. Chem. C **114**, 10512 (2010).
[34]A. Merenda, E. D. Ligneris, K. Sears, T. Chaffraix, K. Magniez, D. Cornu, J. A. Schütz, and L. F. Dumée, Sci. Rep. **6**, 31565 (2016).
[35]K. S. Siow, L. Britcher, S. Kumar, and H. J. Griesser, Plasma Processes Polym. **3**, 392 (2006).
[36]D. Hegemann, Thin Solid Films **581**, 2 (2014).
[37]J. N. Israelachvili and M. L. Gee, Langmuir **5**, 288 (1989).
[38]T. R. Gengenbach, Z. R. Vasic, S. Li, R. C. Chatelier, and H. J. Griesser, Plasmas Polym. **2**, 91 (1997).
[39]R. C. Chatelier, X. Xie, T. R. Gengenbach, and H. J. Griesser, Langmuir **11**, 2576 (1995).
[40]A. Ahmadalinezhad, R. Tailor, and A. Sayari, Chem. Eur. J. **19**, 10543 (2013).